CHAPTER

Force and Stress

4

Chapter 3 investigated the kinematics of continuum deformation regardless of the force or stress distribution that produced the motion or deformation. In this chapter, we now wish to examine how these forces and stresses can be quantitatively described. Following the classical continuum mechanics model, we assume a continuously distributed internal force system composed of body and surface forces. Each of these will be associated with a continuous density function that will represent the force per unit volume or per unit surface area. For surface forces, this will lead to the definition and use of the *stress or traction vector* and *stress tensor*. Each of these provides a quantitative method to describe both boundary and internal force distributions within a continuum. Since stress is related to force per unit area, we will have to keep track of whether we wish to use reference or current areas for large deformation problems. Stress is very important in continuum mechanics applications, because many materials exhibit some type of failure condition based on this variable. It should be noted that the developments in this chapter will not require a material constitutive assumption and thus they will apply to a broad class of material behavior.

4.1 BODY AND SURFACE FORCES

When a continuum material is subjected to applied external loadings, internal forces are induced inside the body. Following our continuum philosophy, we assume that these internal forces are distributed continuously within the material. In order to study such forces, it is convenient to categorize them into two major groups, commonly referred to as *body forces* and *surface forces*.

Body forces are proportional to the body's mass and are reacted with an agent *outside* the body. Examples of these include gravitational-weight forces, magnetic forces, and inertial forces. Fig. 4.1A shows an example body force of an object's self-weight producing a particular deformation. Using continuum mechanics principles, a *body force density* (force per unit mass) $\boldsymbol{b}(\boldsymbol{x}, t)$ can be defined such that the total resultant body force $\boldsymbol{F}_R$ of an entire object can be written as a volume integral over the body B:

$$\boldsymbol{F}_R = \iiint_B \rho \boldsymbol{b}(\boldsymbol{x}, t)\, dV \tag{4.1.1}$$

where ρ is the mass density of the material. Later in the text, we will often use the *body force per unit volume* defined by $\boldsymbol{F} = \rho \boldsymbol{b}$.

Continuum Mechanics Modeling of Material Behavior. http://dx.doi.org/10.1016/B978-0-12-811474-2.00004-6

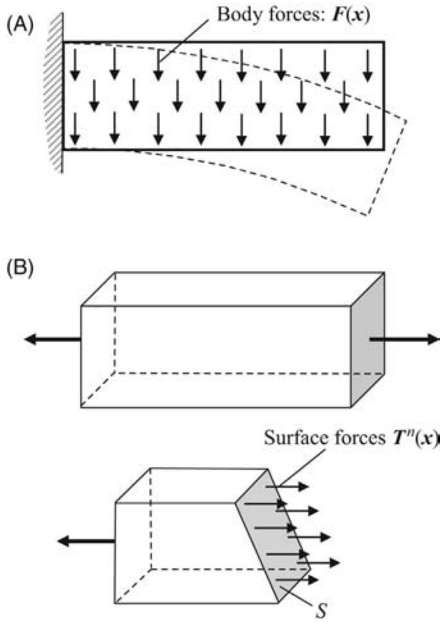

FIGURE 4.1

Examples of body and surfaces forces: (A) cantilever beam under self-weight loading; (B) sectioned axially loaded structure.

Surface forces always act on a surface and result from physical contact with another body. Fig. 4.1B illustrates surface forces existing in a structural solid section that has been created by sectioning the body into two pieces. For this particular case, the surface S is a virtual one in the sense that it was artificially created to investigate the nature of the internal forces at this location in the body. Again, the resultant surface force $\boldsymbol{F}_S$ over an entire surface S can be expressed as the integral of a *surface force density function* $\boldsymbol{t}(\boldsymbol{x}, t)$:

$$\boldsymbol{F}_S = \iint_S \boldsymbol{t}(\boldsymbol{x}, t)\, dS \tag{4.1.2}$$

The surface force density is normally referred to as the *traction or stress vector* and will be discussed in more detail in the next section. We assume *a priori* that the body force density $\boldsymbol{b}$ and the traction $\boldsymbol{t}$ are objective vectors. These density variables can be functions of both position and time, but in the future we will generally drop writing the time dependence.

In the development of classical continuum mechanics, distributions of body or surface couples are normally not included. Theories which include such force system distributions have been constructed in an effort to extend the classical theory for applications in micromechanical modeling. Such approaches include *micropolar* or *couple-stress theory* (see Eringen, 1968) and will be further explored in Chapter 9.

4.2 CAUCHY STRESS PRINCIPLE: STRESS VECTOR

In order to quantify the nature of the internal distribution of forces within a continuum, consider a general body subject to arbitrary (concentrated and distributed) external loadings as shown in Fig. 4.2. For now, we will assume that the body is in its current deformed configuration. To investigate the internal forces, a section is made through the body as shown. On this section, consider a small area Δa with a unit normal vector $\boldsymbol{n}$. In general, the resultant of the surface forces acting on Δa would be a force $\Delta \boldsymbol{F}$ and a moment $\Delta \boldsymbol{M}$. We now wish to determine the pointwise value of the force per unit area and thus the *stress* or *traction vector* is defined by

$$\boldsymbol{t}(\boldsymbol{x},t,\boldsymbol{n}) = \lim_{\Delta a \to 0} \frac{\Delta \boldsymbol{F}}{\Delta a} \tag{4.2.1}$$

For the resultant moment case, we assume that in the limit

$$\lim_{\Delta a \to 0} \frac{\Delta \boldsymbol{M}}{\Delta a} = 0 \tag{4.2.2}$$

which is consistent with our earlier discussion that no resultant surface couple will be included in classical continuum mechanics.

Notice that the traction vector depends on both the spatial location and the unit normal vector to the surface under study. Thus, even though we may be investigating the same point, the traction vector will still vary as a function of the orientation of the surface normal. This concept is often called the *Cauchy Stress Principle* which can be stated as *the stress or traction vector at any given place and time has a same value*

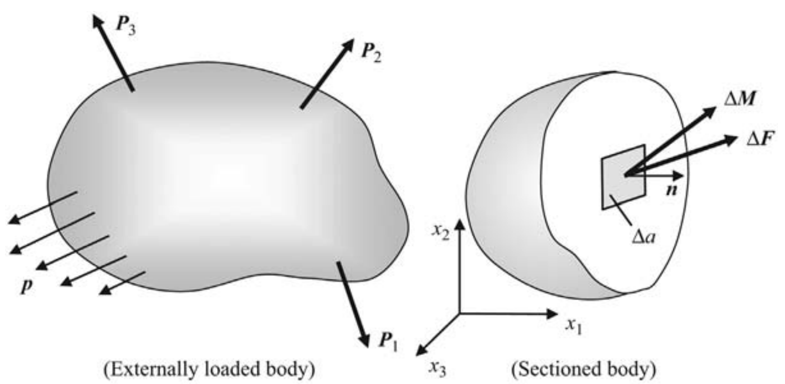

FIGURE 4.2

Stress vector concept.

on all parts of material having a common tangent plane and lying on the same side of it. Note also the expected action–reaction principle (Newton's third law) which is often expressed as

$$t(\boldsymbol{x},\boldsymbol{n}) = -\boldsymbol{t}(\boldsymbol{x},-\boldsymbol{n}) \tag{4.2.3}$$

4.3 CAUCHY STRESS TENSOR

Consider now the special case where the small area Δa (shown in Fig. 4.2) coincides with each of the three coordinate planes with unit normal vectors pointing along the positive coordinate axes. This concept is shown in Fig. 4.3 where the three coordinate surfaces partition off a cube of material. For this case, the traction vector on each face can be written as

$$\begin{aligned}\boldsymbol{t}(\boldsymbol{x},\boldsymbol{n}=\boldsymbol{e}_1) &= T_{11}\boldsymbol{e}_1 + T_{12}\boldsymbol{e}_2 + T_{13}\boldsymbol{e}_3 \\ \boldsymbol{t}(\boldsymbol{x},\boldsymbol{n}=\boldsymbol{e}_2) &= T_{21}\boldsymbol{e}_1 + T_{22}\boldsymbol{e}_2 + T_{23}\boldsymbol{e}_3 \\ \boldsymbol{t}(\boldsymbol{x},\boldsymbol{n}=\boldsymbol{e}_3) &= T_{31}\boldsymbol{e}_1 + T_{32}\boldsymbol{e}_2 + T_{33}\boldsymbol{e}_3\end{aligned} \tag{4.3.1}$$

where $\boldsymbol{e}_1$, $\boldsymbol{e}_2$, and $\boldsymbol{e}_3$ are the coordinate unit vectors, and the nine quantities T_{11}, T_{22}, T_{33}, T_{12}, T_{21}, T_{23}, T_{32}, T_{31}, and T_{13} are the components of the traction vector on each of the three coordinate planes as illustrated. These nine components are called the *Cauchy stress components*, with T_{11}, T_{22}, and T_{33} being referred to as *normal stresses* and T_{12}, T_{21}, T_{23}, T_{32}, T_{31}, and T_{13} called the *shearing stresses*. The components of stress T_{ij} are commonly written in a matrix format as

$$T_{ij} = \begin{bmatrix} T_{11} & T_{12} & T_{13} \\ T_{21} & T_{22} & T_{23} \\ T_{31} & T_{32} & T_{33} \end{bmatrix} \tag{4.3.2}$$

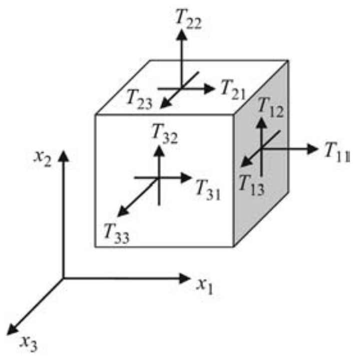

FIGURE 4.3

Traction components on coordinate surfaces—Cauchy stresses.

We will shortly show that this stress is a second-order tensor obeying the appropriate transformation law $(2.8.1)_3$. Since it represents the force per unit area in the deformed or current configuration, T_{ij} is sometimes referred to as the *true stress*. It should be mentioned that in Chapter 5, we will formally prove that the Cauchy stress is a symmetric tensor.

The positive directions of each stress component are illustrated in Fig. 4.3. Regardless of the coordinate system, positive normal stress always acts in tension out of the face, and only one subscript would be necessary for definition since it always acts normal to the surface. The shear stress, however, requires two subscripts, the first representing the plane of action and the second designating the direction of the stress. Similar to shear strain, the sign of the shear stress depends on coordinate system orientation. For example, on a plane with a normal in the positive x_1-direction, positive T_{12} acts in the positive x_2-direction. Similar definitions would follow for the other shear stress components. Proper formulation of continuum mechanics problems will require knowledge of these basic definitions, directions, and sign conventions for particular stress components. Notice that relations (4.3.1) imply that on coordinate boundary surfaces, the components of the traction vector are directly related to particular stress components. This fact will simplify certain boundary conditions and thus lead to a more direct problem solution.

Consider next the tetrahedron element bounded by an oblique plane of arbitrary orientation and three coordinate planes as shown in Fig. 4.4. Appropriate traction loadings exist on each of these surfaces. The unit normal to the oblique surface is given by

$$\boldsymbol{n} = n_1\boldsymbol{e}_1 + n_2\boldsymbol{e}_2 + n_3\boldsymbol{e}_3 \tag{4.3.3}$$

where n_1, n_2, and n_3 are the direction cosines of the unit vector $\boldsymbol{n}$ relative to the given coordinate system. The area of the oblique surface will be denoted by da and thus the areas of each of the coordinate surfaces are given by n_1da, n_2da, and n_3da. We

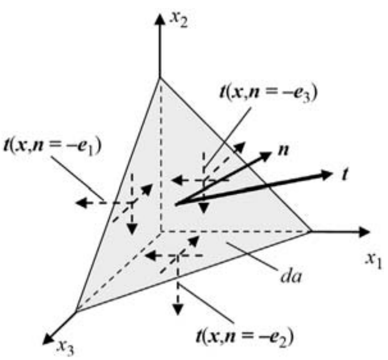

FIGURE 4.4

Tractions on tetrahedron element.

now consider the dynamic equilibrium of the element interior to the oblique and coordinate planes and take the limit as the volume shrinks to zero. Invoking Newton's law, the force balance between the various surface tractions must equal the element's mass times acceleration:

$$\boldsymbol{t}\,da - n_1\,da\,\boldsymbol{t}(\boldsymbol{n}=\boldsymbol{e}_1) - n_2\,da\,\boldsymbol{t}(\boldsymbol{n}=\boldsymbol{e}_2) - n_3\,da\,\boldsymbol{t}(n=\boldsymbol{e}_3) = m\boldsymbol{a} \tag{4.3.4}$$

Note that we have used the fact that $\boldsymbol{t}(\boldsymbol{n}=-\boldsymbol{e}_i)=-\boldsymbol{t}(\boldsymbol{n}=\boldsymbol{e}_i)$. Since the elements mass is proportional to $(da)^{3/2}$, in the limit as element volume goes to zero ($da \to 0$), the inertia term on the right-hand side of relation (4.3.4) will vanish. Thus, using relations (4.3.1), we can solve for the traction vector in terms of the stress components

$$\begin{aligned}\boldsymbol{t} = &(T_{11}n_1 + T_{21}n_2 + T_{31}n_3)\boldsymbol{e}_1\\ &+(T_{12}n_1 + T_{22}n_2 + T_{32}n_3)\boldsymbol{e}_2\\ &+(T_{13}n_1 + T_{23}n_2 + T_{33}n_3)\boldsymbol{e}_3\end{aligned} \tag{4.3.5}$$

or in index and direct notation

$$t_i = T_{ji}n_j, \quad \boldsymbol{t} = \boldsymbol{T}^T\boldsymbol{n} \tag{4.3.6}$$

Relations (4.3.5) and (4.3.6) thus indicate that the stress or traction vector is linearly related to the unit normal vector through a linear transformation using the transpose of the stress tensor. This result is often called the *Cauchy stress formula*. This result provides a simple and direct method to calculate the forces on oblique planes and surfaces and will prove to be very useful to specify general boundary conditions during the formulation and solution of solid mechanics problems.

Next, let us formally show that the Cauchy stress is a second-order tensor. We start with the assumption that the traction and normal vectors are first-order tensors and thus $t_i' = Q_{ij}t_j$ and $n_i' = Q_{ij}n_j$. Starting from (4.3.6) in the primed frame

$$\begin{aligned}&t_i' = T_{ji}'n_j' \Rightarrow Q_{ij}t_j = T_{ji}'Q_{jk}n_k \Rightarrow Q_{ij}T_{kj}n_k = T_{ji}'Q_{jk}n_k \Rightarrow\\ &Q_{im}(Q_{ij}T_{kj} - T_{ji}'Q_{jk})n_k = 0 \Rightarrow T_{km} = Q_{jk}Q_{im}T_{ji}'\end{aligned}$$

The final expression is just the standard tensor transformation law for second-order tensors.

The distinction between the traction vector and stress tensor should be carefully understood. Although each quantity has the same units of force per unit area, they are fundamentally different since the traction is a vector, whereas the stress is a second-order tensor. Components of traction can be defined on any surface, but particular stress components only exist on coordinate surfaces as shown in Fig. 4.3 for the Cartesian case. Eq. (4.3.6) establishes the relation between the two variables, thereby indicating that each traction component can be expressed as a linear combination of particular stress components. Further discussion on this topic will be given later in Chapter 6 when boundary condition development is presented.

EXAMPLE 4.3.1 FOR THE GIVEN STATE OF STRESS $T_{ij} = \begin{bmatrix} 1 & 2 & 2 \\ 2 & 3 & 4 \\ 2 & 4 & 6 \end{bmatrix}$, **DETERMINE THE TRACTION VECTOR ON A PLANES WITH UNIT NORMAL VECTORS** $n^{(1)} = \frac{1}{\sqrt{3}}(e_1 + e_2 + e_3)$ **AND** $n^{(2)} = \frac{1}{\sqrt{2}}(e_1 + e_2)$.

Solution: Using (4.3.6)

$$t_i^{(1)} = T_{ji}n_j^{(1)} = \frac{1}{\sqrt{3}}\begin{bmatrix} 1 & 2 & 2 \\ 2 & 3 & 4 \\ 2 & 4 & 6 \end{bmatrix}\begin{bmatrix} 1 \\ 1 \\ 1 \end{bmatrix} = \frac{1}{\sqrt{3}}\begin{bmatrix} 5 \\ 9 \\ 12 \end{bmatrix},$$

$$t_i^{(2)} = T_{ji}n_j^{(2)} = \frac{1}{\sqrt{2}}\begin{bmatrix} 1 & 2 & 2 \\ 2 & 3 & 4 \\ 2 & 4 & 6 \end{bmatrix}\begin{bmatrix} 1 \\ 1 \\ 0 \end{bmatrix} = \frac{1}{\sqrt{2}}\begin{bmatrix} 3 \\ 5 \\ 6 \end{bmatrix}$$

The Cauchy stress components follow the standard transformation rules for second-order tensors established in Section 2.8. Applying transformation relation $(2.8.1)_3$ for the stress gives

$$T'_{ij} = Q_{ip}Q_{jq}T_{pq} \tag{4.3.7}$$

where the rotation matrix $Q_{ij} = \cos(x'_i, x_j)$. Therefore, given the stress in one coordinate system, we can determine the new components in any other rotated system. This will be a very handy tool for many problems in continuum mechanics. For the general three-dimensional case, the rotation matrix may be chosen in the form

$$Q_{ij} = \begin{bmatrix} l_1 & m_1 & n_1 \\ l_2 & m_2 & n_2 \\ l_3 & m_3 & n_3 \end{bmatrix} \tag{4.3.8}$$

Using this notational scheme, the specific transformation relations for the stress then become

$$\begin{aligned}
T'_{11} &= T_{11}l_1^2 + T_{22}m_1^2 + T_{33}n_1^2 + 2(T_{12}l_1m_1 + T_{23}m_1n_1 + T_{31}n_1l_1) \\
T'_{22} &= T_{11}l_2^2 + T_{22}m_2^2 + T_{33}n_2^2 + 2(T_{12}l_2m_2 + T_{23}m_2n_2 + T_{31}n_2l_2) \\
T'_{33} &= T_{11}l_3^2 + T_{22}m_3^2 + T_{33}n_3^2 + 2(T_{12}l_3m_3 + T_{23}m_3n_3 + T_{31}n_3l_3) \\
T'_{12} &= T_{11}l_1l_2 + T_{22}m_1m_2 + T_{33}n_1n_2 + T_{12}(l_1m_2 + m_1l_2) + T_{23}(m_1n_2 + n_1m_2) + T_{31}(n_1l_2 + l_1n_2) \\
T'_{23} &= T_{11}l_2l_3 + T_{22}m_2m_3 + T_{33}n_2n_3 + T_{12}(l_2m_3 + m_2l_3) + T_{23}(m_2n_3 + n_2m_3) + T_{31}(n_2l_3 + l_2n_3) \\
T'_{31} &= T_{11}l_3l_1 + T_{22}m_3m_1 + T_{33}n_3n_1 + T_{12}(l_3m_1 + m_3l_1) + T_{23}(m_3n_1 + n_3m_1) + T_{31}(n_3l_1 + l_3n_1)
\end{aligned} \tag{4.3.9}$$

For the two-dimensional case, the transformation matrix reduces to

$$Q_{ij} = \begin{bmatrix} \cos\theta & \sin\theta \\ -\sin\theta & \cos\theta \end{bmatrix} \tag{4.3.10}$$

with θ being the counterclockwise angle defined in Fig. 2.9. Under this transformation, the in-plane stress components transform according to

$$
\begin{aligned}
T'_{11} &= T_{11}\cos^2\theta + T_{22}\sin^2\theta + 2T_{12}\sin\theta\cos\theta \\
T'_{22} &= T_{11}\sin^2\theta + T_{22}\cos^2\theta - 2T_{12}\sin\theta\cos\theta \\
T'_{12} &= -T_{11}\sin\theta\cos\theta + T_{22}\sin\theta\cos\theta + T_{12}(\cos^2\theta - \sin^2\theta)
\end{aligned}
\tag{4.3.11}
$$

which is commonly rewritten in terms of the double angle

$$
\begin{aligned}
T'_{11} &= \frac{T_{11}+T_{22}}{2} + \frac{T_{11}-T_{22}}{2}\cos 2\theta + T_{12}\sin 2\theta \\
T'_{22} &= \frac{T_{11}+T_{22}}{2} - \frac{T_{11}-T_{22}}{2}\cos 2\theta - T_{12}\sin 2\theta \\
T'_{12} &= \frac{T_{22}-T_{11}}{2}\sin 2\theta + T_{12}\cos 2\theta
\end{aligned}
\tag{4.3.12}
$$

Both two- and three-dimensional stress transformation equations can be easily incorporated within MATLAB to provide numerical solution to problems of interest.

4.4 PRINCIPAL STRESSES AND AXES FOR CAUCHY STRESS TENSOR

We can again use the previous developments from Section 2.11 to discuss the issues of principal stresses and directions. As mentioned, it will be shown later that the Cauchy stress is a symmetric tensor. Using this fact, appropriate theory has been developed to determine the principal axes and values for the stress. For any given Cauchy stress tensor, we can establish the principal value problem and solve the characteristic equation to explicitly determine the principal values and directions. The general characteristic equation for this case becomes

$$
\det[T_{ij} - T\delta_{ij}] = -T^3 + I_T T^2 - II_T T + III_T = 0 \tag{4.4.1}
$$

where T are the *principal stresses* and the fundamental invariants are given by

$$
\begin{aligned}
I_T &= T_{ii} = T_{11} + T_{22} + T_{33} \\
II_T &= \frac{1}{2}(T_{ii}T_{jj} - T_{ij}T_{ij}) = \begin{vmatrix} T_{11} & T_{12} \\ T_{21} & T_{22} \end{vmatrix} + \begin{vmatrix} T_{22} & T_{23} \\ T_{32} & T_{33} \end{vmatrix} + \begin{vmatrix} T_{11} & T_{13} \\ T_{31} & T_{33} \end{vmatrix} \\
III_T &= \det \boldsymbol{T}
\end{aligned}
\tag{4.4.2}
$$

In the principal coordinate system, the stress matrix will take the special diagonal form

$$
T_{ij} = \begin{bmatrix} T_1 & 0 & 0 \\ 0 & T_2 & 0 \\ 0 & 0 & T_3 \end{bmatrix} \tag{4.4.3}
$$

The fundamental invariants can be expressed in terms of the three principal stresess T_1, T_2, and T_3 as

$$\begin{aligned} I_T &= T_1 + T_2 + T_3 \\ II_T &= T_1T_2 + T_2T_3 + T_3T_1 \\ III_T &= T_1T_2T_3 \end{aligned} \tag{4.4.4}$$

A comparison of the general and principal stress states are shown in Fig. 4.5. Notice that for the principal coordinate system, all shearing stresses will vanish and thus the state will only have normal stresses.

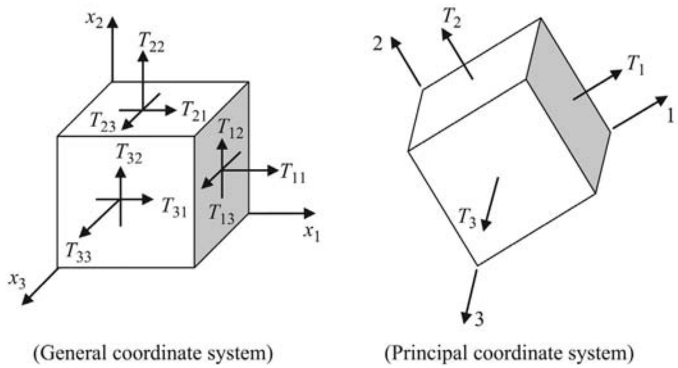

FIGURE 4.5

Comparison of general and principal stress states.

EXAMPLE 4.4.1 CAUCHY STRESS PRINCIPAL VALUE PROBLEM

Determine the principal stresses and directions for the given state of stress,

$$T_{ij} = \begin{bmatrix} 3 & 1 & 1 \\ 1 & 0 & 2 \\ 1 & 2 & 0 \end{bmatrix}.$$

Solution: The principal stress problem is started by calculating the three invariants, giving the result $I_T = 3$, $II_T = -6$, $III_T = -8$. This yields the following characteristic equation:

$$-T^3 + 3T^2 + 6T - 8 = 0$$

The roots of this equation are found to be $T = 4, 1, -2$. Back-substituting the first root into the fundamental system (2.11.1) gives

$$\begin{aligned} -n_1^{(1)} + n_2^{(1)} + n_3^{(1)} &= 0 \\ n_1^{(1)} - 4n_2^{(1)} + 2n_3^{(1)} &= 0 \\ n_1^{(1)} + 2n_2^{(1)} - 4n_3^{(1)} &= 0 \end{aligned}$$

Solving this system, the normalized principal direction is found to be $\boldsymbol{n}^{(1)} = (2, 1, 1)/\sqrt{6}$. In a similar fashion, the other two principal directions are $\boldsymbol{n}^{(2)} = (-1, 1, 1)/\sqrt{3}$, $\boldsymbol{n}^{(3)} = (0, -1, 1)/\sqrt{2}$.

We now wish to go back to investigate another issue related to stress and traction transformation that makes use of principal stresses. Consider the general traction vector $\boldsymbol{t}$ acting on an arbitrary surface as shown in Fig. 4.6. The issue of interest is to determine the traction vector's normal and shear components N and S. The normal component is simply the traction's projection in the direction of the unit normal vector $\boldsymbol{n}$, whereas the shear component is found by Pythagorean theorem:

$$\begin{aligned} N &= \boldsymbol{t}\cdot\boldsymbol{n} \\ S &= \left(|\boldsymbol{t}|^2 - N^2\right)^{1/2} \end{aligned} \tag{4.4.5}$$

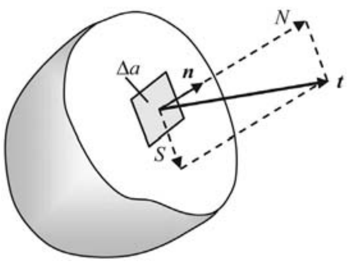

FIGURE 4.6

Traction vector decomposition.

Using the relationship for the traction vector (4.3.6) into $(4.4.5)_1$ gives

$$\begin{aligned} N &= \boldsymbol{t}\cdot\boldsymbol{n} = t_i n_i = T_{ji} n_j n_i \\ &= T_1 n_1^2 + T_2 n_2^2 + T_3 n_3^2 \end{aligned} \tag{4.4.6}$$

where in order to simplify the expressions, we have used the principal axes for the stress tensor. In a similar manner,

$$\begin{aligned} |\boldsymbol{t}|^2 &= \boldsymbol{t}\cdot\boldsymbol{t} = t_i t_i = T_{ji} n_j T_{ki} n_k \\ &= T_1^2 n_1^2 + T_2^2 n_2^2 + T_3^2 n_3^2 \end{aligned} \tag{4.4.7}$$

Using these results in relations (4.4.5) yields

$$\begin{aligned} N &= T_1 n_1^2 + T_2 n_2^2 + T_3 n_3^2 \\ S^2 + N^2 &= T_1^2 n_1^2 + T_2^2 n_2^2 + T_3^2 n_3^2 \end{aligned} \tag{4.4.8}$$

In addition, we also add the condition that the vector $\boldsymbol{n}$ has unit magnitude

$$1 = n_1^2 + n_2^2 + n_3^2 \tag{4.4.9}$$

Relations (4.4.8) and (4.4.9) can be viewed as three linear algebraic equations for the unknowns n_1^2, n_2^2, n_3^2. Solving this system gives the following result:

$$
\begin{aligned}
n_1^2 &= \frac{S^2 + (N - T_2)(N - T_3)}{(T_1 - T_2)(T_1 - T_3)} \\
n_2^2 &= \frac{S^2 + (N - T_3)(N - T_1)}{(T_2 - T_3)(T_2 - T_1)} \\
n_3^2 &= \frac{S^2 + (N - T_1)(N - T_2)}{(T_3 - T_1)(T_3 - T_2)}
\end{aligned} \tag{4.4.10}
$$

Without loss in generality, we can rank the principal stresses as $T_1 > T_2 > T_3$. Noting that the expressions given by (4.4.10) must be greater than or equal to zero, we can conclude the following:

$$
\begin{aligned}
S^2 + (N - T_2)(N - T_3) \geq 0 \\
S^2 + (N - T_3)(N - T_1) \leq 0 \\
S^2 + (N - T_1)(N - T_2) \geq 0
\end{aligned} \tag{4.4.11}
$$

For the equality case, Eqs. (4.4.11) represent three circles in an S–N coordinate system, and Fig. 4.7 illustrates the location of each circle. These results were originally generated by Otto Mohr over a century ago, and the circles are commonly called *Mohr's circles of stress*. The three inequalities given in (4.4.11) imply that all admissible values of N and S lie in the shaded regions bounded by the three circles. Note that for the ranked principal stresses, the largest shear component is easily determined as $S_{max} = ½\left|T_1 - T_3\right|$. Although these circles can be effectively used for two-dimensional stress transformation, the general tensorial-based equations (4.3.7) or (4.3.9) are normally used for general transformation computations.

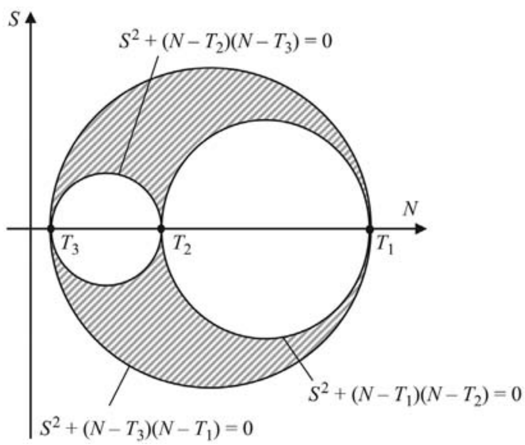

FIGURE 4.7

Mohr's circles of stress.

4.5 SPHERICAL, DEVIATORIC, OCTAHEDRAL, AND VON MISES STRESS

Similar to our earlier discussion on strain, it is often convenient to decompose the stress into two parts called the *spherical* and *deviatoric stress tensors*. Analogous to relations given in Chapter 3, the spherical Cauchy stress is defined by

$$\tilde{T}_{ij} = \frac{1}{3} T_{kk} \delta_{ij} \tag{4.5.1}$$

whereas the deviatoric stress becomes

$$\hat{T}_{ij} = T_{ij} - \frac{1}{3} T_{kk} \delta_{ij} \tag{4.5.2}$$

Note that the total stress is then simply the sum

$$T_{ij} = \tilde{T}_{ij} + \hat{T}_{ij} \tag{4.5.3}$$

The spherical stress is an isotropic tensor, being the same in all coordinate systems (as per discussion in Section 2.15). Using the fact that the characteristic equation for the deviatoric stress reduces to

$$\hat{T}^3 + II_{\hat{T}} \hat{T} - III_{\hat{T}} = 0 \tag{4.5.4}$$

it can be shown that the principal directions of the deviatoric stress are the same as those of the stress tensor itself (see Exercise 4.13).

We next briefly explore a couple of particular stress components or combinations that have been defined in the literature and are commonly used in formulating failure theories related to inelastic deformation. It has been found that ductile materials normally exhibit inelastic yielding failures that can be characterized by these particular stresses. Consider first the normal and shear stresses (tractions) that act on a special plane whose normal makes equal angles with the three principal axes. This plane is commonly referred to as the *octahedral plane*. Determination of these stresses is straight forward if we use the principal axes of stress. Since the unit normal vector to the octahedral plane makes equal angles with the principal axes, its components are given by $n_i = \pm(1,1,1)/\sqrt{3}$. Referring to Fig. 4.6 and using the results of the previous section, relations (4.4.8) give the desired normal and shear stresses as

$$\begin{aligned} N = \sigma_{oct} &= \frac{1}{3}(T_1 + T_2 + T_3) = \frac{1}{3} T_{kk} = \frac{1}{3} I_T \\ S = \tau_{oct} &= \frac{1}{3}\left[(T_1 - T_2)^2 + (T_2 - T_3)^2 + (T_3 - T_1)^2\right]^{1/2} \\ &= \frac{1}{3}\left(2I_T^2 - 6II_T\right)^{1/2} \end{aligned} \tag{4.5.5}$$

It can be shown that the octahedral shear stress τ_{oct} is directly related to the *distortional strain energy* (defined in Chapter 6) which is often used in failure theories for ductile materials.

Another specially defined stress also related to the distortional strain energy failure criteria is known as the *effective* or *von Mises stress* and is given by the expression

$$\begin{aligned}\sigma_e = \sigma_{von\ Mises} &= \sqrt{\frac{3}{2}\hat{T}_{ij}\hat{T}_{ij}} \\ &= \frac{1}{\sqrt{2}}\left[(T_{11}-T_{22})^2+(T_{22}-T_{33})^2+(T_{33}-T_{11})^2+6\left(T_{12}^2+T_{23}^2+T_{31}^2\right)\right]^{1/2} \\ &= \frac{1}{\sqrt{2}}\left[(T_1-T_2)^2+(T_2-T_3)^2+(T_3-T_1)^2\right]^{1/2}\end{aligned} \tag{4.5.6}$$

Note that although the von Mises stress is not really a particular stress or traction component in the usual sense, it is directly related to the octahedral shear stress by the relation $\sigma_e = \left(3/\sqrt{2}\right)\tau_{oct}$. If at some point in the structure, the von Mises stress equals the tensile yield stress, then the material is considered to be at the failure condition. Because of this fact, many finite-element computer codes commonly plot von Mises stress distributions based on the numerically generated stress field. It should be noted that the von Mises and octahedral shear stresses involve only the *differences* in the principal stresses and not the individual values. Thus, increasing each principal stress by the same amount will not change the value of σ_e or τ_{oct}. This result also implies that these values are independent of the hydrostatic stress. The interested reader on failure theories is referred to Ugural and Fenster (2003) for further details on this topic. It should be pointed out that the spherical, octahedral, and von Mises stresses are all expressible in terms of the stress invariants and thus are independent of the coordinate system used to calculate them.

4.6 STRESS DISTRIBUTIONS AND CONTOUR LINES

Over the years, the stress analysis community has developed a large variety of schemes to help visualize and understand the nature of the stress distribution in solids. While stress has been the common pursuit, similar graphical analysis has also been made of strain and displacement distribution. Much of this effort is aimed at determining the magnitude and location of maximum stresses within the structure. Simple schemes involve just plotting the distribution of particular stress components along chosen directions within the body under study. Other methods focus on constructing contour plots of principal stress, maximum shear stress, von Mises stress, and other stress variables or combinations. Some techniques have been constructed to compare with optical experimental methods that provide photographic data of particular stress variables (Shukla and Dally, 2010).

We now will briefly explore some of these schemes as they relate to two-dimensional *plane stress distributions* defined in the x_1–x_2 plane by the field:

$$T_{11} = T_{11}(x_1, x_2),\quad T_{22} = T_{22}(x_1, x_2),\quad T_{12} = T_{12}(x_1, x_2),\quad T_{13} = T_{23} = T_{33} = 0 \tag{4.6.1}$$

Note for this case, the principal stresses and maximum shear stress are given in Exercise 4.6. By passing polarized light through transparent model samples under load, the experimental method of *photoelasticity* can provide full field photographic stress data of particular stress combinations. The method can generate *isochromatic* fringe patterns that represent lines of constant difference in the principal stresses, that is, $T_1 - T_2 =$ constant, which would also be lines of maximum shearing stress. An example of an isochromatic fringe pattern is shown in Fig. 4.8 which illustrates a disk under opposite diametrical compressive loadings. Photoelasticity can also generate another series of fringe lines called *isoclinics* along which the principal stresses have a constant orientation. Still another set of contour lines often used in optical experimental stress analysis are *isopachic* contours, which are lines of $T_{11} + T_{22} = T_1 + T_2 =$ constant. These contours are related to the out-of-plane strain and displacement.

An additional, useful set of lines are *isostatics*; they are also referred to as *stress trajectories*. Such lines are oriented along the direction of a particular principal stress. For the two-dimensional plane stress case, the principal stresses T_1 and T_2 give rise to two families of stress trajectories that form an orthogonal network composed of lines free of shear stress. These trajectories have proved to be useful aids for understanding load paths, that is, how external loadings move through a solid continuum structure to the reaction points (Kelly and Tosh, 2000). Stress trajectories are also related to structural optimization, and Michell structures composed of frameworks of continuous members in tension and compression (Dewhurst, 2001). Additional two-dimensional contour plots of stress function derivatives have also been proposed in the literature (Rathkjen, 1997).

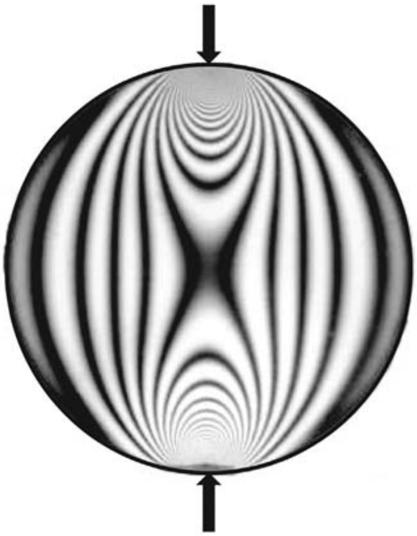

(Courtesy of Dynamic Photomechanics Laboratory, University of Rhode Island)

FIGURE 4.8

Photoelastic isochromatic contours for a disk under diametrical compression.

Considering a particular stress trajectory, the orientation angle θ_p with respect to the x_1-axis can be found using the relation

$$\tan 2\theta_p = \frac{2T_{12}}{T_{11} - T_{22}} \tag{4.6.2}$$

Now replacing x_1, x_2 with x, y, for a given trajectory specified by $y(x)$, $\tan\theta_p = \frac{dy}{dx}$ and combining these results with a standard trigonometric identity gives

$$\tan 2\theta_p = \frac{2\tan\theta_p}{1-\tan^2\theta_p} = \frac{2\dfrac{dy}{dx}}{1-\left(\dfrac{dy}{dx}\right)^2} = \frac{2T_{12}}{T_{11}-T_{22}}$$

This relation is easily solved for the trajectory slope

$$\frac{dy}{dx} = -\frac{T_{11}-T_{22}}{2T_{12}} \pm \sqrt{1+\left(\frac{T_{11}-T_{22}}{2T_{12}}\right)^2} \tag{4.6.3}$$

So given in-plane stress components, the differential equation (4.6.3) can be integrated to generate the stress trajectories, $y(x)$. Although some special cases can be done analytically (Molleda et al., 2005), most stress distributions will generate complicated forms that require numerical integration (Breault, 2012). A particular example will now be explored, and several of the previously discussed stress contours and lines are generated and plotted.

EXAMPLE 4.6.1 ELASTIC STRESS DISTRIBUTIONS IN A DISK UNDER DIAMETRICAL COMPRESSION

Consider a specific two-dimensional problem of a circular disk loaded by equal but opposite concentrated forces along a given diameter as shown in Fig. 4.9A. Sadd (2014) provides the linear elastic solution to this problem, and with respect to the given axes the in-plane stresses are found to be

$$\begin{aligned}
T_{11} &= -\frac{2P}{\pi}\left[\frac{(R-y)x^2}{r_1^4} + \frac{(R+y)x^2}{r_2^4} - \frac{1}{2R}\right] \\
T_{22} &= -\frac{2P}{\pi}\left[\frac{(R-y)^3}{r_1^4} + \frac{(R+y)^3}{r_2^4} - \frac{1}{2R}\right] \\
T_{12} &= \frac{2P}{\pi}\left[\frac{(R-y)^2 x}{r_1^4} - \frac{(R+y)^2 x}{r_2^4}\right]
\end{aligned} \tag{4.6.4}$$

where $r_{1,2} = \sqrt{x^2 + (R \mp y)^2}$. Numerical results are presented for the case with unit radius and unit loading ($R = 1$, $P = 1$). For this case, Fig. 4.9 illustrates

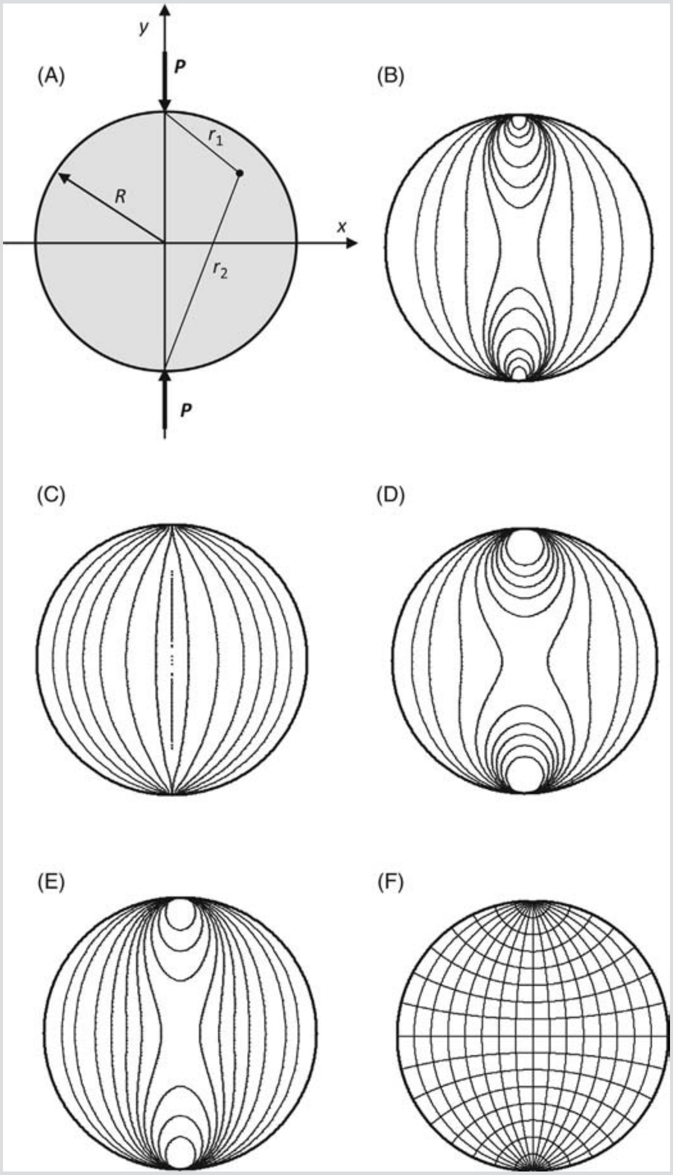

FIGURE 4.9

Elastic stress contours for diametrically loaded disk problem: (A) disk problem; (B) maximum shear stress contours (isochromatic lines); (C) maximum principal stress contours; (D) sum of principal stress contours (isopachic lines); (E) von Mises stress contours; (F) stress trajectories (isostatic lines).

several contour distributions and the stress trajectories that have been previously discussed. It should be apparent that each of these contour distributions is, in general, different from one another and each will convey particular information about the nature of the stress field under study.

4.7 REFERENCE CONFIGURATION PIOLA–KIRCHHOFF STRESS TENSORS

As discussed in Chapter 3, under finite deformations the reference area and current deformed area will not be the same (see Section 3.7). This difference must then be reconciled in the definitions of the stress tensor. Recall that the Cauchy stress previously discussed was an Eulerian variable defined as the force per unit area in the current deformed configuration. This stress tensor is widely used in many fields of continuum mechanics. However, there are particular cases where it will be advantageous to formulate the problem in the reference configuration in which certain variables will be known. For example, choosing the initial configuration as reference, we might know some features about the problem geometry when things begin. We now wish to explore the stress in the Lagrangian context, that is, the force per unit area in the reference configuration, and this will lead to two new and different stress tensors.

We start by reviewing the situation shown in Fig. 4.10 which illustrates the traction and normal vectors on an arbitrary differential area in both the reference and current configurations. As previously described in Section 4.2, the traction vector in the current configuration is denoted by $\boldsymbol{t}$ and the area on which it acts is da with unit normal vector $\boldsymbol{n}$. In the reference configuration, this differential area is dA with unit normal $\boldsymbol{N}$, and the traction vector in this configuration is designated as $\boldsymbol{T}^R$. Note that traction $\boldsymbol{T}^R$ is often referred to as a *pseudo*-vector since it represents the force in the current configuration but is evaluated per unit area in the undeformed reference configuration. It is important to realize what is different and what is the same between

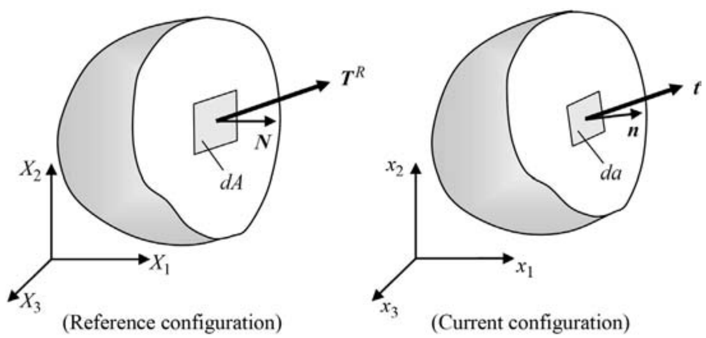

FIGURE 4.10

Reference and current differential areas and tractions.

the two configurations. Clearly, the areas and the unit normals are different since there is kinematic deformation between the two configurations. However, the total force acting on each area is to be the same and thus we can write

$$\boldsymbol{T}^R \, dA = \boldsymbol{t} \, da \tag{4.7.1}$$

Reviewing this relation, we note that the two traction vectors $\boldsymbol{t}$ and $\boldsymbol{T}^R$ act in the same direction with different magnitudes. Following a similar (but not identical) scheme used for the Cauchy stress tensor (4.3.6), we define a *Lagrangian stress tensor* T^o_{ij} as

$$T^R_i = T^o_{ij} N_j \tag{4.7.2}$$

T^o_{ij} is commonly called the *first Piola–Kirchhoff (PK1) stress tensor*. Note that relation (4.7.2) differs from (4.3.6) by using the form T^o_{ij} and not the transpose T^o_{ji}.

Combining (4.3.6) and (4.7.2) in (4.7.1) then expresses the common force relation as

$$T^o_{ij} N_j \, dA = T_{ji} n_j \, da \tag{4.7.3}$$

Going back to Section 3.7, the changes in the areas were given by Nanson's formula (3.7.3):

$$\boldsymbol{n} \, da = J(\boldsymbol{F}^{-1})^T \boldsymbol{N} \, dA \tag{4.7.4}$$

where $J = \det F$ is the Jacobian of the deformation. Using this result in (4.7.3) yields

$$T^o_{ij} N_j \, dA = T_{ji} J F^{-1}_{kj} N_k \, dA \Rightarrow (T^o_{ik} - T_{ji} J F^{-1}_{kj}) N_k = 0$$

thus resulting in the equation relating the PK1 stress to the Cauchy stress:

$$\begin{aligned} T^o_{ij} &= J F^{-1}_{jk} T_{ki} = J F^{-1}_{jk} T_{ik} \\ \boldsymbol{T}^o &= J \boldsymbol{T} \left(\boldsymbol{F}^{-1}\right)^T \end{aligned} \tag{4.7.5}$$

This relation can be easily inverted to express the Cauchy stress in terms of the PK1 stress:

$$T_{ij} = J^{-1} F_{jk} T^o_{ik}, \quad \boldsymbol{T} = J^{-1} \boldsymbol{T}^o \boldsymbol{F}^T \tag{4.7.6}$$

We have used the fact that the Cauchy stress will be shown to be symmetric. Exploring the symmetry of the PK1 stress tensor, we take the transpose of (4.7.5) to get

$$T^o_{ji} = J F^{-1}_{ik} T_{kj} = J F^{-1}_{ik} T_{jk} \neq T^o_{ij}$$

and thus the first Piola–Kirchhoff stress tensor T^o_{ij} is not, in general, symmetric even with a symmetric Cauchy stress. Note that some authors define a *nominal stress* $\boldsymbol{N}$ as the transpose of the PK1 stress, that is, $\boldsymbol{N} = \boldsymbol{T}^{o^T}$.

A second reference stress tensor may be developed by evaluating the force in the reference configuration using a pull-back operation as discussed in Section 3.6. Similar to the relation $d\boldsymbol{X} = \boldsymbol{F}^{-1}\,d\boldsymbol{x}$, we can express the force acting on dA as

$$\begin{gathered}\boldsymbol{SN}\,dA = \boldsymbol{F}^{-1}\boldsymbol{t}\,da = \boldsymbol{F}^{-1}(\boldsymbol{T}^{o}\boldsymbol{N}\,dA) \Rightarrow \\ \boldsymbol{S} = \boldsymbol{F}^{-1}\boldsymbol{T}^{o}\end{gathered} \tag{4.7.7}$$

where we have used relation (4.7.3), and $\boldsymbol{S}$ is the new stress called the *second Piola–Kirchhoff stress tensor* (PK2). Using (4.7.5), we can express PK2 in terms of the Cauchy stress as

$$S_{ij} = JF_{il}^{-1}F_{jk}^{-1}T_{lk}, \quad \boldsymbol{S} = J\boldsymbol{F}^{-1}\boldsymbol{T}(\boldsymbol{F}^{-1})^{T} \tag{4.7.8}$$

Checking the symmetry property of S_{ij} gives

$$S_{ji} = JF_{jl}^{-1}F_{ik}^{-1}T_{lk} = JF_{ik}^{-1}F_{jl}^{-1}T_{kl} = S_{ij}$$

and thus the second Piola–Kirchhoff stress is symmetric if the Cauchy stress is symmetric. It is a simple exercise to determine the Cauchy stress in terms of the PK2 stress:

$$T_{ij} = J^{-1}F_{ik}F_{jl}S_{kl}, \quad \boldsymbol{T} = J^{-1}\boldsymbol{FSF}^{\mathrm{T}} \tag{4.7.9}$$

For small deformations $\nabla\boldsymbol{u} \approx \mathrm{O}(\varepsilon)$, where $\varepsilon \ll 1$. This situation implies the following:

$$\begin{aligned}&\boldsymbol{F} = \boldsymbol{I} + \nabla\boldsymbol{u} \approx \boldsymbol{I} + \mathrm{O}(\varepsilon)\\ &\boldsymbol{F}^{-1} = \boldsymbol{I} - \nabla\boldsymbol{u}^{*} \approx \boldsymbol{I} - \mathrm{O}(\varepsilon)\\ &J = \det\boldsymbol{F} \approx 1 + \mathrm{O}(\varepsilon)\\ &\boldsymbol{T}^{o} = J\boldsymbol{T}\left(\boldsymbol{F}^{-1}\right)^{T} \approx \boldsymbol{T}\\ &\boldsymbol{S} = J\boldsymbol{F}^{-1}\boldsymbol{T}\left(\boldsymbol{F}^{-1}\right)^{T} \approx \boldsymbol{T}\end{aligned}$$

Thus, for small deformations, both Piola–Kirchhoff stress tensors reduce to the Cauchy stress.

EXAMPLE 4.7.1 DETERMINATION OF PIOLA–KIRCHHOFF STRESS TENSORS

For a Cauchy stress state $T_{ij} = \begin{bmatrix} 3 & 1 & 0 \\ 1 & 2 & 0 \\ 0 & 0 & 0 \end{bmatrix}$, under simple shearing deformation, determine the PK1 and PK2 stress tensors. Next, calculate the pseudo-stress vector $\boldsymbol{T}^{R}$ acting on a plane with unit normal $\boldsymbol{e}_1$ associated with PK1 and PK2.

Solution: For simple shearing deformation,

$$\boldsymbol{F} = \frac{\partial\boldsymbol{x}}{\partial\boldsymbol{X}} = \begin{bmatrix} 1 & \gamma & 0 \\ 0 & 1 & 0 \\ 0 & 0 & 1 \end{bmatrix}, \quad \boldsymbol{F}^{-1} = \frac{\partial\boldsymbol{X}}{\partial\boldsymbol{x}} = \begin{bmatrix} 1 & -\gamma & 0 \\ 0 & 1 & 0 \\ 0 & 0 & 1 \end{bmatrix}, \quad J = 1$$

For PK1, use (4.7.5) ⇒

$$\boldsymbol{T}^{o} = J\boldsymbol{T}(\boldsymbol{F}^{-1})^{T} = \begin{bmatrix} 3 & 1 & 0 \\ 1 & 2 & 0 \\ 0 & 0 & 0 \end{bmatrix} \begin{bmatrix} 1 & 0 & 0 \\ -\gamma & 1 & 0 \\ 0 & 0 & 1 \end{bmatrix} = \begin{bmatrix} 3-\gamma & 1 & 0 \\ 1-2\gamma & 2 & 0 \\ 0 & 0 & 0 \end{bmatrix}$$

For PK2, use (4.7.7) ⇒

$$\boldsymbol{S} = \boldsymbol{F}^{-1}\boldsymbol{T}^{o} = \begin{bmatrix} 1 & -\gamma & 0 \\ 0 & 1 & 0 \\ 0 & 0 & 1 \end{bmatrix} \begin{bmatrix} 3-\gamma & 1 & 0 \\ 1-2\gamma & 2 & 0 \\ 0 & 0 & 0 \end{bmatrix} = \begin{bmatrix} 3-2\gamma+2\gamma^{2} & 1-2\gamma+ & 0 \\ 1-2\gamma & 2 & 0 \\ 0 & 0 & 0 \end{bmatrix}$$

Note that PK2 is symmetric, whereas PK1 is not.
Now using (4.7.2) with $\boldsymbol{N} = \boldsymbol{e}_1$, traction associated with PK1 is thus

$$\boldsymbol{T}^{R} = \boldsymbol{T}^{o}\boldsymbol{N} = \begin{bmatrix} 3-\gamma & 1 & 0 \\ 1-2\gamma & 2 & 0 \\ 0 & 0 & 0 \end{bmatrix} \begin{bmatrix} 1 \\ 0 \\ 0 \end{bmatrix} = \begin{bmatrix} 3-\gamma \\ 1-2\gamma \\ 0 \end{bmatrix}$$

and similarly from (4.7.7), the traction related to PK2 is

$$\boldsymbol{SN} = \begin{bmatrix} 3-2\gamma+2\gamma^{2} & 1-2\gamma+ & 0 \\ 1-2\gamma & 2 & 0 \\ 0 & 0 & 0 \end{bmatrix} \begin{bmatrix} 1 \\ 0 \\ 0 \end{bmatrix} = \begin{bmatrix} 3-2\gamma+2\gamma^{2} \\ 1-2\gamma \\ 0 \end{bmatrix}$$

4.8 OTHER STRESS TENSORS

Over the years, several other stress tensors have been defined by the continuum mechanics community. Normally these definitions have particular advantages in special applications. In contrast to the Cauchy and Piola–Kirchhoff stresses, most of these special stress components do not have a direct physical interpretation.

KIRCHHOFF STRESS

The *Kirchhoff stress tensor* is defined in terms of the Cauchy stress by

$$\tau = J\boldsymbol{T} \tag{4.8.1}$$

This stress is sometimes used in plasticity theories and it will occasionally simplify particular equation forms.

BIOT STRESS

The Biot or Jaumann stress tensor is defined as

$$\boldsymbol{T}^{B} = \boldsymbol{R}^{T}\boldsymbol{T}^{o} \tag{4.8.2}$$

where $\boldsymbol{R}$ is the rotation tensor from the polar decomposition of the deformation gradient, $\boldsymbol{F} = \boldsymbol{RU}$, and $\boldsymbol{T}^{o}$ is the first Piola–Kirchhoff stress. This tensor form is useful because it is the energy conjugate (see Section 5.6) to the right stretch tensor $\boldsymbol{U}$. From (4.7.7), $\boldsymbol{T}^o = \boldsymbol{FS}$ and thus (4.8.2) can be written as

$$\boldsymbol{T}^B = \boldsymbol{R}^T\boldsymbol{FS} = \boldsymbol{US} \tag{4.8.3}$$

COROTATIONAL CAUCHY STRESS

For some applications, we may be interested in the stress at an intermediate rotated configuration. The *corotational Cauchy stress* $\boldsymbol{T}^C$ is related to this concept and is given by

$$\boldsymbol{T}^C = \boldsymbol{R}^T\boldsymbol{TR} \tag{4.8.4}$$

where $\boldsymbol{R}$ is an orthogonal rotation tensor. Using (4.7.9), relation (4.8.4) can be expressed in terms of the PK2 stress and the right stretch tensors

$$\boldsymbol{T}^C = J^{-1}\boldsymbol{R}^T\boldsymbol{FSF}^T\boldsymbol{R} = J^{-1}\boldsymbol{USU} \tag{4.8.5}$$

Although a few more specialized stress examples exist, they are not widely used and we will end our discussion on this topic.

4.9 OBJECTIVITY OF STRESS TENSORS

Recalling our objectivity discussions from Sections 1.2, 2.9, 3.5, and 3.6, we now wish to do an objectivity check on the various second-order stress tensors previously presented. For second-order tensors, the $\boldsymbol{Q}$-objectivity test was specified by relation (2.9.3), and thus a general tensor $\boldsymbol{A}$ would have to satisfy the relation $\boldsymbol{A}^* = \boldsymbol{QAQ}^T$. Also collecting some previous results from Section 3.5, we found that the deformation gradient and its inverse satisfied relations $\boldsymbol{F}^* = \boldsymbol{QF}$ and $\boldsymbol{F}^{*-1} = \boldsymbol{F}^{-1}\boldsymbol{Q}^T$.

Starting with the Cauchy stress, we begin with relation (4.3.6), $\boldsymbol{t} = \boldsymbol{T}^T\boldsymbol{n}$. We assume that from their fundamental definitions, vectors $\boldsymbol{n}$ and $\boldsymbol{t}$ are objective and transform as first-order tensors, and thus

$$\begin{aligned}
&\boldsymbol{t} = \boldsymbol{T}^T\boldsymbol{n} \Rightarrow \boldsymbol{Q}^T\boldsymbol{t}^* = \boldsymbol{T}^T\boldsymbol{Q}^T\boldsymbol{n}^* \Rightarrow \boldsymbol{t}^* = \boldsymbol{QT}^T\boldsymbol{Q}^T\boldsymbol{n}^* \\
&\text{but} \quad \boldsymbol{t}^* = \boldsymbol{T}^{*T}\boldsymbol{n}^* \Rightarrow \boldsymbol{T}^{*T}\boldsymbol{n}^* = \boldsymbol{QT}^T\boldsymbol{Q}^T\boldsymbol{n}^* \Rightarrow \\
&\boldsymbol{T}^{*T} = \boldsymbol{QT}^T\boldsymbol{Q}^T \Rightarrow \boldsymbol{T}^* = \boldsymbol{QTQ}^T
\end{aligned} \tag{4.9.1}$$

and thus the Cauchy stress tensor is objective.

Next, let us explore the first Piola–Kirchhoff stress $\boldsymbol{T}^o$. From (4.7.5),

$$\begin{aligned}
&\boldsymbol{T}^{o^*} = J^*\boldsymbol{T}^*\left(\boldsymbol{F}^{*^{-1}}\right)^T \Rightarrow \boldsymbol{T}^{o^*} = J\boldsymbol{QTQ}^T\left(\boldsymbol{F}^{-1}\boldsymbol{Q}^T\right)^T \Rightarrow \\
&\boldsymbol{T}^{o^*} = J\boldsymbol{QTQ}^T\boldsymbol{Q}\left(\boldsymbol{F}^{-1}\right)^T = J\boldsymbol{QT}\left(\boldsymbol{F}^{-1}\right)^T = \boldsymbol{QT}^o
\end{aligned} \tag{4.9.2}$$

We conclude that the first Piola–Kirchhoff stress tensor satisfies the objectivity test for first-order tensors but not for second-order tensors.

Moving on to the PK2 stress $\boldsymbol{S}$, we start with relation (4.7.7):

$$\boldsymbol{S}^* = \boldsymbol{F}^{*-1}\boldsymbol{T}^{*o} = \boldsymbol{F}^{-1}\boldsymbol{Q}^T\boldsymbol{Q}\boldsymbol{T}^o = \boldsymbol{F}^{-1}\boldsymbol{T}^o = \boldsymbol{S} \tag{4.9.3}$$

and thus the second Piola–Kirchhoff stress tensor is the same in both reference frames, and so it is not an objective second-order tensor.

In regard to the Kirchhoff stress $\boldsymbol{\tau} = J\boldsymbol{T}$, since the Cauchy stress is objective and J is a scalar, the Kirchhoff stress is objective. For the Biot stress, using (4.8.3) $\boldsymbol{T}^B = \boldsymbol{U}\boldsymbol{S}$, we can argue that since $\boldsymbol{S}$ and $\boldsymbol{U}^2$ remain the same under the frame change, then $\boldsymbol{T}^B$ will also remain the same and thus will not be an objective second-order tensor. Finally, in light of (4.8.5), the corotational Cauchy stress also remains the same under the $\boldsymbol{Q}$-transformation and thus does not satisfy objectivity for a second-order tensor.

4.10 CYLINDRICAL AND SPHERICAL COORDINATE CAUCHY STRESS FORMS

As discussed in Chapter 3, in order to solve many continuum mechanics problems, formulation must be done in curvilinear coordinates typically using cylindrical or spherical systems. Thus, following similar methods as used with the strain tensor relations in Chapter 3, we now wish to develop expressions for a few of the basic stress and traction concepts for cylindrical and spherical coordinates.

Cylindrical coordinates were originally presented in Fig. 2.6, and for such a system, the Cauchy stress components are defined on the differential element shown in Fig. 4.11. For this coordinate system, the stress matrix is given by

$$\boldsymbol{T} = \begin{bmatrix} T_{rr} & T_{r\theta} & T_{rz} \\ T_{\theta r} & T_{\theta\theta} & T_{\theta z} \\ T_{zr} & T_{z\theta} & T_{zz} \end{bmatrix} \tag{4.10.1}$$

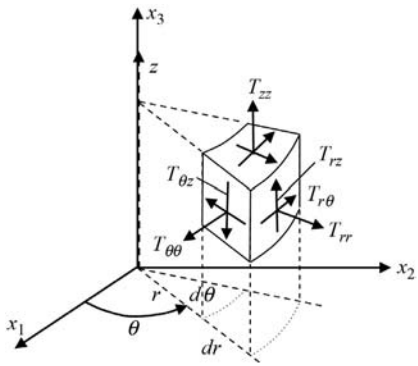

FIGURE 4.11

Stress components in cylindrical coordinates.

Now the stress can be expressed in terms of the traction components as

$$\boldsymbol{T} = \boldsymbol{e}_r \boldsymbol{t}_r + \boldsymbol{e}_\theta \boldsymbol{t}_\theta + \boldsymbol{e}_z \boldsymbol{t}_z \tag{4.10.2}$$

where

$$\begin{aligned} \boldsymbol{t}_r &= T_{rr}\boldsymbol{e}_r + T_{r\theta}\boldsymbol{e}_\theta + T_{rz}\boldsymbol{e}_z \\ \boldsymbol{t}_\theta &= T_{\theta r}\boldsymbol{e}_r + T_{\theta\theta}\boldsymbol{e}_\theta + T_{\theta z}\boldsymbol{e}_z \\ \boldsymbol{t}_z &= T_{zr}\boldsymbol{e}_r + T_{z\theta}\boldsymbol{e}_\theta + T_{zz}\boldsymbol{e}_z \end{aligned} \tag{4.10.3}$$

Next consider these developments for the spherical coordinate system, previously shown in Fig. 2.7. The Cauchy stress components in spherical coordinates are defined on the differential element illustrated in Fig. 4.12, and the stress matrix for this case is

$$\boldsymbol{T} = \begin{bmatrix} T_{RR} & T_{R\phi} & T_{R\theta} \\ T_{\phi R} & T_{\phi\phi} & T_{\phi\theta} \\ T_{\theta R} & T_{\theta\phi} & T_{\theta\theta} \end{bmatrix} \tag{4.10.4}$$

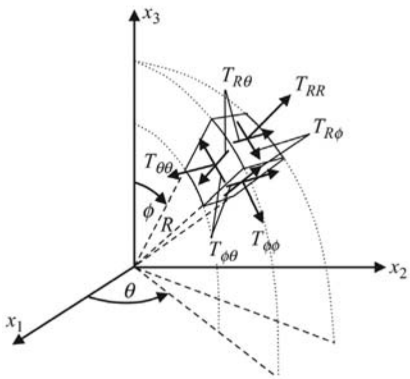

FIGURE 4.12

Stress components in spherical coordinates.

As before, the stress can be expressed in terms of the traction components as

$$\boldsymbol{T} = \boldsymbol{e}_R \boldsymbol{t}_R + \boldsymbol{e}_\phi \boldsymbol{t}_\phi + \boldsymbol{e}_\theta \boldsymbol{t}_\theta \tag{4.10.5}$$

where

$$\begin{aligned} \boldsymbol{t}_R &= T_{RR}\boldsymbol{e}_R + T_{R\phi}\boldsymbol{e}_\phi + T_{R\theta}\boldsymbol{e}_\theta \\ \boldsymbol{t}_\phi &= T_{\phi R}\boldsymbol{e}_R + T_{\phi\phi}\boldsymbol{e}_\phi + T_{\phi\theta}\boldsymbol{e}_\theta \\ \boldsymbol{t}_\theta &= T_{\theta R}\boldsymbol{e}_R + T_{\theta\phi}\boldsymbol{e}_\phi + T_{\theta\theta}\boldsymbol{e}_\theta \end{aligned} \tag{4.10.6}$$

REFERENCES

Breault, B., 2012. Improving load distributions in cellular materials using stress trajectory topology. University of Rhode Island, MS Thesis.

Dewhurst, P., 2001. Analytical solutions and numerical procedures for minimum-weight Michell structures. J. Mech. Phys. Solids 49, 445–467.

Eringen, A.C., 1968. Theory of micropolar elasticity. Liebowitz, H. (Ed.), Fracture, 2, Academic Press, New York, pp. 662–729.

Kelly, D., Tosh, M., 2000. Interpreting load paths and stress trajectories in elasticity. Eng. Comput. 17, 117–135.

Molleda, F., Mora, J., Molleda, F.J., Carrillo, E., Mellor, B.G., 2005. Stress trajectories for mode I fracture. Mater. Characterization 54, 9–12.

Rathkjen, A., 1997. Force lines in plane stress. J. Elasticity 47, 167–178.

Sadd, M.H., 2014. Elasticity theory, applications and numerics, third ed. Elsevier, Waltham, MA.

Shukla, A., Dally, J.W., 2010. Experimental Solid Mechanics. College House Enterprises, Knoxville, TN.

Ugural, A.C., Fenster, S.K., 2003. Advanced strength of materials and applied elasticity. Prentice Hall, Englewood liffs, NJ.

EXERCISES

4.1 For the following Cauchy stress tensors, find the traction vector acting on a plane with the given normal vector $\boldsymbol{n}$. Note that you must first make the normal vector have unit length.

$$(a)\quad \boldsymbol{T}=\begin{bmatrix} 2 & 1 & 1 \\ 1 & 0 & 2 \\ 1 & 2 & 0 \end{bmatrix} \quad (b)\quad \boldsymbol{T}=\begin{bmatrix} 1 & 0 & 1 \\ 0 & 2 & 2 \\ 1 & 2 & 0 \end{bmatrix} \quad (c)\quad \boldsymbol{T}=\begin{bmatrix} 2 & 1 & 0 \\ 1 & 4 & 2 \\ 0 & 2 & 0 \end{bmatrix}$$

$$\boldsymbol{n}=\boldsymbol{e}_1+2\boldsymbol{e}_2+\boldsymbol{e}_3 \qquad \boldsymbol{n}=2\boldsymbol{e}_1+\boldsymbol{e}_2+\boldsymbol{e}_3 \qquad \boldsymbol{n}=\boldsymbol{e}_1+2\boldsymbol{e}_2$$

4.2 For each of the stress tensors in Exercise 4.1, determine the new components in a coordinate frame rotated +90° around the x_1-axis (direction *via* the right-hand rule).

4.3 Explicitly verify the two-dimensional transformation equations (4.3.11) and (4.3.12).

4.4 Show that the general two-dimensional stress transformation relations (4.3.11) can be used to generate relations for the normal and shear stresses in a polar coordinate system in terms of Cartesian components:

$$\begin{aligned} T_{rr} &= T_{11}\cos^2\theta + T_{22}\sin^2\theta + 2T_{12}\sin\theta\cos\theta \\ T_{\theta\theta} &= T_{11}\sin^2\theta + T_{22}\cos^2\theta - 2T_{12}\sin\theta\cos\theta \\ T_{r\theta} &= -T_{11}\sin\theta\cos\theta + T_{22}\sin\theta\cos\theta + T_{12}(\cos^2\theta - \sin^2\theta) \end{aligned}$$

4.5 Verify that the two-dimensional transformation relations giving Cartesian stresses in terms of polar components are given by

$$T_{11} = T_{rr}\cos^2\theta + T_{\theta\theta}\sin^2\theta - 2T_{r\theta}\sin\theta\cos\theta$$
$$T_{22} = T_{rr}\sin^2\theta + T_{\theta\theta}\cos^2\theta - 2T_{r\theta}\sin\theta\cos\theta$$
$$T_{12} = T_{rr}\sin\theta\cos\theta - T_{\theta\theta}\sin\theta\cos\theta + T_{r\theta}(\cos^2\theta - \sin^2\theta)$$

4.6 A two-dimensional state of *plane Cauchy stress* in the x_1,x_2-plane is defined by

$$T_{ij} = \begin{bmatrix} T_{11} & T_{12} & 0 \\ T_{21} & T_{22} & 0 \\ 0 & 0 & 0 \end{bmatrix}$$

Using general principal value theory, show that for this case the in-plane principal stresses and maximum shear stress are given by

$$T_{1,2} = \frac{T_{11} + T_{22}}{2} \pm \sqrt{\left(\frac{T_{11} - T_{22}}{2}\right)^2 + T_{12}^2}$$
$$\tau_{\max} = \sqrt{\left(\frac{T_{11} - T_{22}}{2}\right)^2 + T_{12}^2}$$

4.7 For the plane stress case in Exercise 4.6, demonstrate the invariant nature of the principal stresses and maximum shear stresses by showing that

$$T_{1,2} = \frac{1}{2}I_T \pm \sqrt{\frac{1}{4}I_T^2 - II_T} \text{ and } \tau_{\max} = \sqrt{\frac{1}{4}I_T^2 - II_T}$$

4.8 It was discussed in Section 4.4 that for the case of ranked principal stresses ($T_1 > T_2 > T_3$), the maximum shear stress was given by $S_{\max} = (T_1 - T_3)/2$ which was the radius of the largest Mohr's circle shown in Fig. 4.7. For this case, show that the normal stress acting on the plane of maximum shear is given by $N = (T_1 + T_3)/2$. Finally, using relations (4.4.10), show that the components of the unit normal vector to this plane are $n_i = \pm(1,0,1)/\sqrt{2}$. This result implies that the maximum shear stress acts on a plane that bisects the angle between the directions of the largest and smallest principal stress.

4.9 Explicitly show that the stress state given in Example 4.4.1 will reduce to the proper diagonal form under transformation to principal axes. Follow the transformation scheme shown in Example 2.11.1.

4.10 For the case of *pure shear*, where the stress is given by $\boldsymbol{T} = \begin{bmatrix} 0 & \tau & 0 \\ \tau & 0 & 0 \\ 0 & 0 & 0 \end{bmatrix}$, determine the principal stresses and directions, and compute the normal and shear stress on the octahedral plane.

4.11 For linear elastic materials, stress field solutions can often be written in the general form $T_{ij} = Pf_{ij}(\boldsymbol{x})$, where P is a loading parameter and the tensor function f_{ij} specifies only the field distribution. Show, in general, that for this case, the principal stresses will be a linear form in P, that is, $T_{1,2,3} = Pg_{1,2,3}(\boldsymbol{x})$. Next demonstrate that the principal directions will not depend on P.

4.12 Determine the spherical and deviatoric stress tensors for the Cauchy stress states given in Exercise 4.1.

4.13 Show that the principal directions of the deviatoric Cauchy stress tensor $\hat{\boldsymbol{T}}$ coincide with the principal directions of the stress tensor $\boldsymbol{T}$. Also show that the principal values of the deviatoric stress $\hat{T}_i$ can be expressed in terms of the principal values T_i by the relation $\hat{T}_i = T_i - \frac{1}{3}T_{kk}$. This problem is analogous to Exercise 3.21.

4.14 Show that the second invariant of the Cauchy stress deviator tensor may be written in the following forms:

$$
\begin{aligned}
II_{\hat{T}} &= -\frac{1}{2}\left(\hat{T}_{11}^2 + \hat{T}_{22}^2 + \hat{T}_{33}^2\right) - T_{12}^2 - T_{23}^2 - T_{31}^2 \\
&= -\frac{1}{6}\left[\left(\hat{T}_{11} - \hat{T}_{22}\right)^2 + \left(\hat{T}_{22} - \hat{T}_{33}\right)^2 + \left(\hat{T}_{33} - \hat{T}_{11}\right)^2\right] - T_{12}^2 - T_{23}^2 - T_{31}^2 \\
&= -\frac{1}{6}\left[(T_{11} - T_{22})^2 + (T_{22} - T_{33})^2 + (T_{33} - T_{11})^2\right] T_{12}^2 - T_{23}^2 - T_{31}^2
\end{aligned}
$$

4.15 Show that the second and third invariants of the Cauchy deviatoric stress tensor can be written as

$$
\begin{aligned}
II_{\hat{T}} &= -\frac{1}{2}\left(T_{ij}T_{ij} - \frac{2}{3}I_T^2 + \frac{1}{3}I_T^2\right) = II_T - \frac{1}{3}I_T^2 \\
III_{\hat{T}} &= \frac{1}{3}\operatorname{tr}\hat{\boldsymbol{T}}^3 = \frac{2}{27}I_T^3 - \frac{1}{3}I_T II_T + III_T
\end{aligned}
$$

For the third invariant, make use of the Cayley–Hamilton Theorem.

4.16 Explicitly verify relations (4.5.5) for the octahedral Cauchy stress components. Also assuming that $\boldsymbol{T}$ is symmetric, show that they can be expressed in terms of the general stress components by

$$
\sigma_{oct} = \frac{1}{3}(T_{11} + T_{22} + T_{33})
$$

$$
\tau_{oct} = \frac{1}{3}\left[(T_{11} - T_{22})^2 + (T_{22} - T_{33})^2 + (T_{33} - T_{11})^2 + 6T_{12}^2 + 6T_{23}^2 + 6T_{31}^2\right]^{1/2}
$$

4.17 Determine the von Mises and octahedral stresses for the Cauchy stress states given in Exercise 4.1. Use results in Exercise 4.16 for the octahedral stresses.

4.18 The plane stress solution for a semi-infinite linear elastic solid under a concentrated point loading P (Flamant problem) is given by

$$T_{11} = -\frac{2Px_1^2x_2}{\pi\left(x_1^2+x_2^2\right)^2}$$
$$T_{22} = -\frac{2Px_2^3}{\pi\left(x_1^2+x_2^2\right)^2}$$
$$T_{12} = -\frac{2Px_1x_2^2}{\pi\left(x_1^2+x_2^2\right)^2}$$

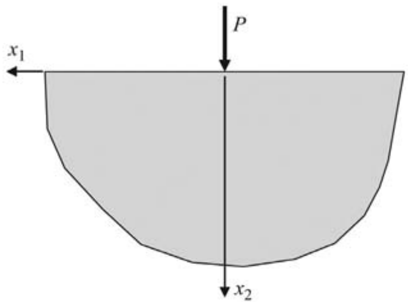

Calculate the maximum shear stress at any point in the body (see Exercise 4.6) and then use MATLAB or equivalent (see example code C-5) to plot contours of $\tau_{\max}$.

4.19 A linear elastic plane stress solution $T_{11} = -\frac{3Px_1x_2}{2c^3} + \frac{N}{2c}, T_{22} = 0, T_{12} = -\frac{3P}{4c}\left(1-\frac{x_2^2}{c^2}\right)$, where P and N are constants, has been determined for the illustrated rectangular domain. Determine the boundary stresses and their resultants (including both forces and moments) that act on each of the four boundaries. These boundary conditions should indicate that this is the solution to a particular beam problem.

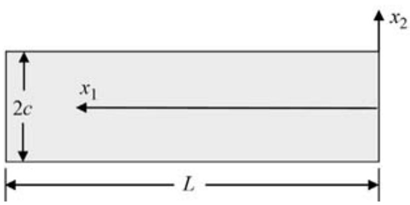

4.20 For each of the stress tensors in Exercise 4.1 under extensional deformation

$$x_1 = \lambda_1 X_1, \quad x_2 = \lambda_2 X_2, \quad x_3 = \lambda_3 X_3$$

determine the first and second Piola–Kirchhoff stress tensors. Check that PK2 is symmetric.

4.21 Consider the isochoric extensional deformation $x_1 = 2X_1, x_2 = X_2/\sqrt{2}, x_3 = X_3/\sqrt{2}$ of a long bar whose axis lies along the x_1-direction and has unit square cross-section in the reference configuration. First, determine the change in cross-sectional area from the reference to the current configuration. Next, if the Cauchy stress is to be taken as uniaxial,

$\boldsymbol{T} = T_{11}\boldsymbol{e}_1\boldsymbol{e}_1$, calculate the first and second Piola–Kirchhoff stress tensors. Compare the 11-components of each of the three stress tensors.

4.22 Consider uniaxial extensional deformation of a material only along the x_1-direction. Transverse deformation is constrained and so $x_1 = \lambda X_1, x_2 = X_2, x_3 = X_3$. If the Cauchy stress is to be taken as uniaxial, $\boldsymbol{T} = T_{11}\boldsymbol{e}_1\boldsymbol{e}_1$, calculate the first and second Piola–Kirchhoff stress tensors.